ACS APPLIED MATERIALS & INTERFACES

Research Article

www.acsami.org

Nanotransfer Molding of Free-Standing Nanowire and Porous Nanomembranes Suspended on Microtrenches

Dae-Geun Choi,*[†,‡] Ki-Joong Lee,[†] and Jung Yup Kim[†]

[†]Nano-Mechanical Systems Research Division, Korea Institute of Machinery & Materials (KIMM), 171 Jang-dong, Yuseong-gu, Daejeon, 305-343, Republic of Korea

[‡]Department of Nano-Mechatronics, University of Science and Technology, 217 Gajungro, Yuseong-gu, Daejeon, 305-350, Republic of Korea

Supporting Information

ABSTRACT: Direct transfer printing of functional materials has been employed in the development of sensors, displays, and energy-harvesting devices. The transfer process can be applied advantageously to depositions onto nonplanar and flexible surfaces at low temperatures. In this work, we fabricated free-standing nanowire arrays and nanomembranes on micrometer-scale trenches by nanotransfer molding. We also investigated how deposition pattern types vary with trench dimensions as well as processing pressure and temperature. Finally, a free-standing polymer membrane fabricated by nanotransfer molding was employed as a novel mask in the preparation of three-dimensional nanodot arrays.

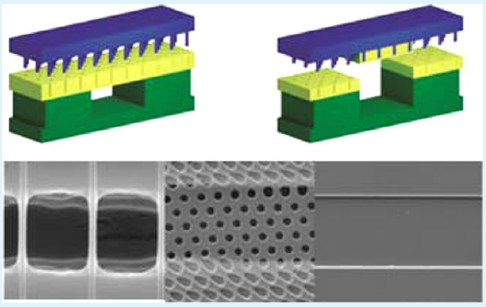

KEYWORDS: *transfer printing, free-standing, nanowire, nanomembrane, nanostencil, shadow mask, molding, reverse imprint*

1. INTRODUCTION

Among the various unconventional nanopatterning methods that include nanoimprinting,[1] capillary force lithography,[2] and transfer printing,[3,4] direct transfer printing (DTP) is particularly promising as it can be used for the deposition of a diverse range of materials on flexible, nonplanar, or patterned surfaces. Nanotransfer-molding (NTM) or printing is a type of DTP method that has been widely pursued as a low-cost, high-throughput, and contamination-free process for the transfer of metals,[5−8] semiconductors,[9−15] and functional polymers.[16−22] NTM can advantageously be performed at low temperature, without deformation of flexible polymer substrates, and without the need for wet chemical treatments or severe plasma etching, rendering the process particularly suitable for organic systems. Owing to such versatility, NTM techniques have found use in a number of device applications including inorganic light-emitting diodes (LEDs),[10] nanogenerators,[12] compound semiconductor transistors,[13] silicon photodiodes,[14] organic solar cells,[23−26] organic thin film transistors (OTFTs),[27] OLEDs,[28] microlens arrays,[29] and three-dimensional microstructure transfer.[30]

The fabrication of free-standing nanofilms or nanowires suspended over micrometer-sized trenches is very important in the fundamental studies of investigating the intrinsic mechanical or electrical properties in nanoscale because any disturbance induced by substrate's surface can be excluded in the free-standing structures.[31,32] Also, the free-standing nanostructures have been widely studied because of their potential applications in field-effect transistors (FETs),[33] mechanical- or electromechanical- resonators,[34−36] and nanoswitch.[37]

Recently, laterally free-standing nanowire arrays have been prepared from the solution deposition of suspended nanowires onto electron-beam lithographically patterned substrates.[36,37] The reported methodologies, however, cannot be scaled, thus hindering their commercial viability. Another interesting approach, albeit with limited position and alignment control, employs dielectrophoresis to align nanowires. A further drawback of this process is that it can only be applied to conductive materials and requires the use of patterned electrodes.[38,39] Recently, directional sliding and contact printing were suggested as means for lateral transfer of vapor phase vertically grown nanowires onto desired substrates.[40,41] Although materials arising from the aforementioned methodologies exhibit interesting properties, no method to date is capable of fabricating free-standing nanowires with precise position and density control, uniform diameter, and perfect alignment on microtrenches and still a systematic study of aligned polymer nanowires or nanomembranes on microtrenches is lacking. In addition, the nanopatterning of polymers or oxide-based nanostructures with weak mechanical strength on microstructured trenches or patterned substrates by conventional photolithography using wet chemical treatment or dry etching remains significantly challenging.

Received: October 29, 2012
Accepted: December 18, 2012
Published: December 18, 2012

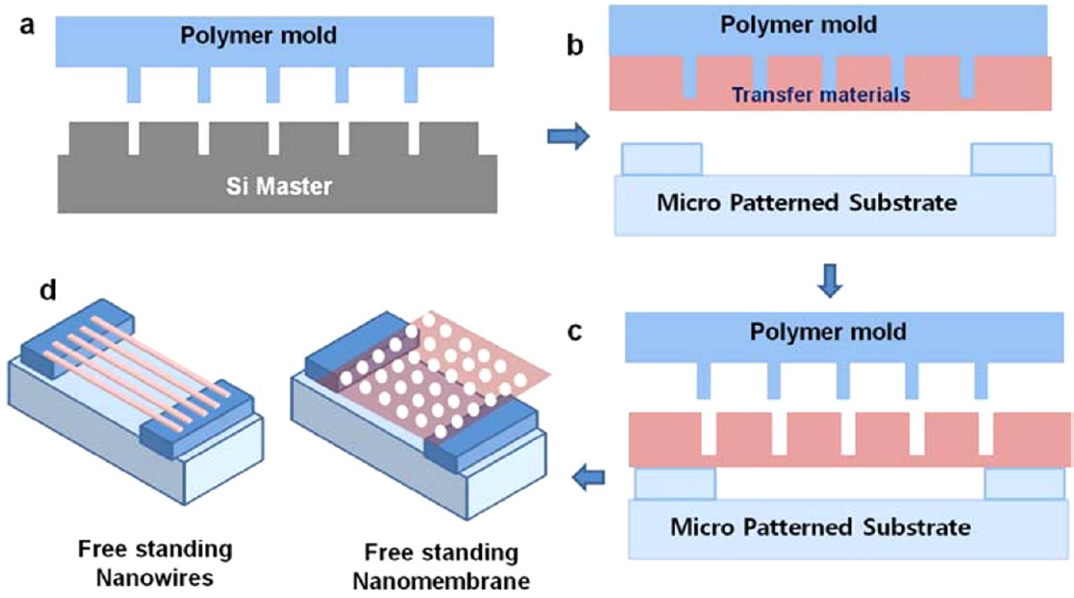

Figure 1. Schemes of NTMonMT process using a polymer mold. (a) polymer mold replicated from Si master. (b) Spin-coating of functional transfer materials. (c) Nanostructured film transferred by the NTM process on a microtrench. (d) Final free-standing nanowires and nanomembrane following post-treatment.

In this work, free-standing nanowires and nanomembranes were fabricated on microtrenches by nanotransfer molding (NTM). With this method, aligned polymer and zinc oxide (ZnO) nanowires were prepared on microtrenches. The effect of processing conditions on deposition patterns was investigated. Finally, pyramidal three-dimensional (3D) metal dot arrays that are inaccessible through conventional lift-off processes were successfully fabricated using a NTM-prepared free-standing porous polymer membrane on a microtrench as a nanoshadow mask (or stencil mask).

2. EXPERIMENTAL SECTION

Materials. Poly(methylmethacrylate)(PMMA) resins (495 PMMA A6) were purchased from Micro Resist Technology (Berlin, Germany) and used as received. For the fabrication of a flexible poly(urethane acrylate) (PUA) mold,[6,18] a urethane acrylate oligomer (Ebercryl 284) was purchased from SK Cytec Co. (Seoul, Korea). Tri(propylene glycol) diacrylate as a monomer and 2,2-dimethoxy-2-phenyl-acetophenon as a photoinitiator were purchased from Sigma-Aldrich (St. Louis, MO, USA). The mixing ratio of oligomer, monomer, and photoinitiator was 2.7:21.3:1.0. A UV-curable silicone additive (Rad 2200N, TEGO Chemie Service) was added to the resin mixture at a ratio of 1 wt % to 5 wt % to promote the release property of the PUA mold. For the fabrication of perfluoropolyether (PFPE) mold,[9] a UV-curable PFPE oligomer (MD 700) was purchased from Solvay Solexis (Ballate, Italy). For the fabrication of zinc(Zn) containing inorganic resin,[42] zinc acetate as a monomer, 2-methylethanol as a solvent, ethanolamine as a stabilizer, and 2-nitrobenzaldehyde as a cross-linker were purchased from Sigma-Aldrich (St. Louis, MO, USA) and mixed with ratio of 1.7: 12: 0.5:1.7.

Fabrication of Micrometer-Scale Silicon Trenches and Silicon Nanomasters. Trenches of various gap size and micrometer scale depth were fabricated by photolithography and a silicon etching process (NNFC in Korea). Silicon masters were prepared for line patterning and nanoporous membrane fabrication, respectively. The former line-master consisted of lines with widths of 200 nm and pitches of 1 μm. The latter hole-master consisted of hexagonal arrays of holes of 265 nm diameter and pitch of 530 nm. The surface of silicon was treated with air plasma for improved adhesion.

NTMonMT Process. Nanostructured films, isolated free-standing nanowires, and porous nanomembranes were transferred by the NTM process onto microtrenches (NTMonMT) and subsequently subjected to post-treatment at an appropriate pressure and temperature (Figure 1). The NTM process can be performed at low temperature and low pressure. In fact, the process pressure can be varied from millibars to several tens of bars. As shown in Figure 2, various transfer or deposition patterns including a continuous free-standing film, a selectively transferred structure on the trench surfaces, a continuous nanostructured film with recessed areas, and complex patterns with partially nontransferred areas can all be created using the NTMonMT process.

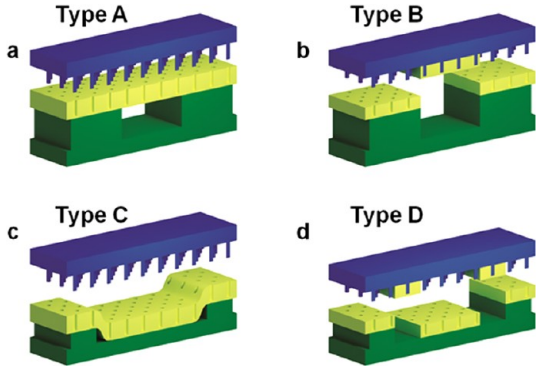

Figure 2. Schemes of various NTMonMT transfer types. (a) Type A structures consist of a continuous free-standing film with nanostructures on the trench. (b) Type B corresponds to a structure selectively transferred onto the surface of trenches. (c) Type C forms a continuous nanostructured film with a recessed area at the bottom of the trenches. (d) Type D consists of complex patterns having partially nontransferred areas near the edge of the trenches.

Fabrication of Free-Standing Polymer Nanowires and Nanomembranes by NTMonMT. Flexible PUA molds with a water contact angle of 85° were replicated from Si masters by UV(365 nm) curing at an intensity of 30 mW/cm^2 for a duration of 120 s. PMMA resin (495 PMMA A6 for 350 nm thickness) was then spin-coated onto the nanopatterned PUA molds at a spin-rate of 3000 rpm. The PMMA-coated PUA mold was then pressed onto the trenches with micrometer-scale gaps at various temperatures in the range of 90 °C for low temperature below glass-transition temperature (T_g) ~ 150

dx.doi.org/10.1021/am302493x | ACS Appl. Mater. Interfaces 2013, 5, 418−424

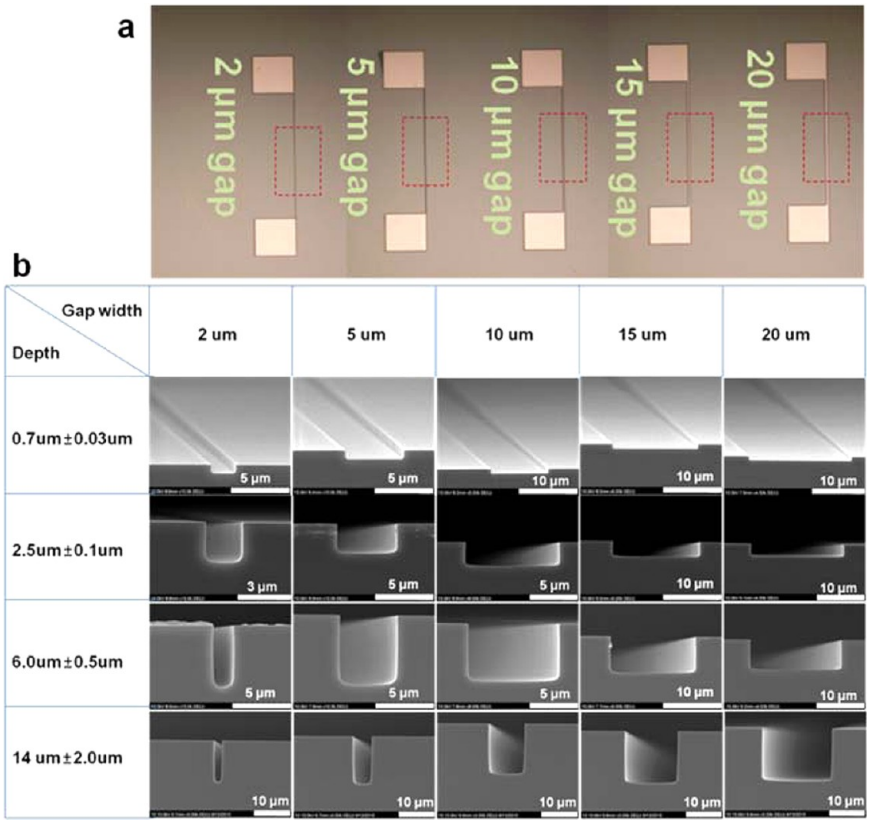

Figure 3. (a) Digital camera images of micrometer-scale silicon trenches with various gap widths. (b) SEM images and detailed dimensional analysis of the silicon trenches used in this work.

°C for high temperature. Pressures were changed from 6 bar for low pressure to 20 bar for high pressure. To isolate the free-standing PMMA nanowires, the residual PMMA layer was removed by O_2 plasma etching for 30 s at a power of 100 W and a pressure of 100 sccm.

Fabrication of Free-Standing ZnO Nanowire Arrays by NTMonMT. A PFPE mold replicated from a Si master with line shape of widths of 200 nm (pitches of 1 μm) was used as the polymer mold for NTMonMT-fabricated ZnO nanowire arrays. The Zn containing inorganic resin consisting of zinc acetate was spin-coated onto the PFPE mold at a spin rate of 4500 rpm.[42] The NTMonMT process was performed at a temperature of 110 °C and a pressure of 6 bar for a duration of 2 min. Following the NTMonMT process, the nanoline patterns were calcined at 300 °C for 60 min in a muffle furnace to afford isolated free-standing ZnO nanowire arrays.

3D Metal Dot Arrays Using Free-Standing Shadow Mask. For the fabrication of the pyramidal 3D metal dot arrays, 500 nm of Cr was deposited by e-beam evaporation through a free-standing polymer membrane mask suspended on microtrenches. The polymer membrane mask was removed using adhesive tape for scanning electron microscopy analysis.

SEM Characterization. Nanostructured patterns were imaged by field-emission scanning electron microscopy (FE-SEM, an FEI Sirion 200).

3. RESULTS AND DISCUSSION

Images of micrometer-scale silicon trenches with various gap widths used in this work were shown in Figure 3. Free standing polymer line patterns with nanometer dimensions and isolated nanowire arrays were prepared by NTMonMT. This transfer method is a dry process as it does not require the use of selective dissolution of sacrificial layers or solvent-assisted adhesion control (Figure 4).

Free-Standing Polymer Nanowires. The effect of trench gap-width on transfer pattern type (i.e., Type A, B, C, or D) was investigated under varying processing conditions. At pressures above 20 bar and temperatures below the polymer T_g, Type A patterns (Figure 2a) were obtained on 2.0 μm narrow gaps. As shown in images a and b in Figure 4, Type C behavior dominated when wider gaps of 20 μm were employed. However, at 6 bar and a temperature of 90 °C (i.e., below T_g), Type A patterns were observed on both 2.0 and 20 μm gaps. After transfer printing, isolated nanolines along the 2.0 μm (Figure 4c) and 20 μm (Figure 4d) gaps could be successfully obtained upon O_2 reactive ion plasma etching, which removes the residual pattern layer of PMMA. The width of PMMA nanolines was reduced from 200 to 90 nm following O_2 etching (see Figure 4c). Long PMMA nanolines deposited on 20 μm gaps (Figure 4d) collapsed during plasma etching because of van der Waals interaction between PMMA lines and mechanical strain induced by gas flow within the plasma chamber. In this work, UV-cured polymer molds such as PUA and PFPE were employed instead of the widely used poly(dimethylsiloxane) (PDMS). High cross-link density and thus, high mechanical strength as well as high resistance to organic solvents can be achieved with PUA and PFPE as compared to PDMS molds, which are easily swollen by contact with organic solvents.

Free-Standing ZnO Nanowires. ZnO semiconductor nanowire assemblies are promising for applications such as chemical sensors and TFTs.[36,37,39] As shown in Figure 5a, ZnO nanoline patterns of 200 nm width and 1.0 μm pitch could be transferred onto 2 μm microchannels by the NTM process. When extremely narrow gaps such as 2 μm microchannels were

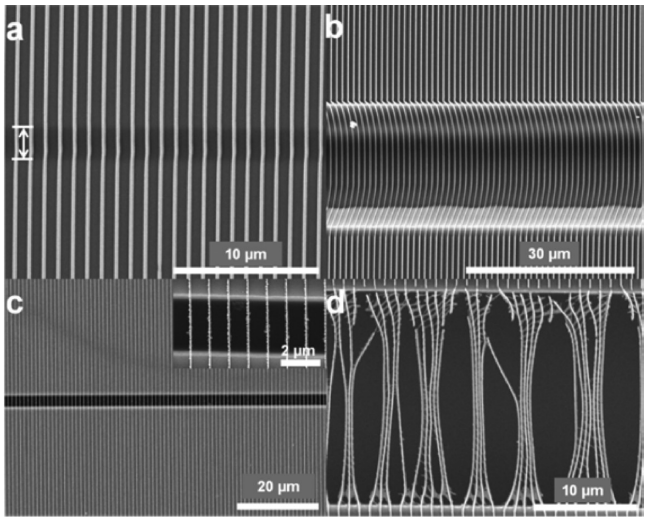

Figure 4. (a, b) SEM images of PMMA nanoline patterns with a residual layer several tens of nanometers in thickness prepared by NTMonMT at a pressure of 20 bar. (a) Free-standing PMMA line patterns on silicon trenches with 2 μm gaps (Type A in the case of Figure 2). (b) Continuous PMMA nanoline patterns in contact with a recessed area at the bottom of the silicon trenches with 20 μm gaps (Type C in case of Figure 2). (c, d) SEM images of isolated free-standing PMMA nanowires prepared by NTMonMT at a pressure of 6.0 bar with subsequent O_2 plasma etching to isolate each nanoline. (c) Free-standing PMMA nanowire arrays with perfect ordering and short length on trenches with 2 μm gaps. (d) Free-standing long PMMA nanowire arrays with bent and cut regions on trenches with 20 μm gaps. Inset of c shows an enlarged image of the isolated PMMA nanolines. The depth of the silicon trenches was approximately 2.5 μm. Transfer temperature was 90 °C, which was below the T_g of PMMA.

used, Type A ZnO structures as shown in images a and b in Figure 5 resulted. Type B patterns were observed with ZnO on intermediate gaps from 5 to 20 μm regardless of the processing temperature and pressure (Figure 5c). When wide gaps are employed, Type D patterns may also be observed (not shown here). However, Type C patterns were challenging to obtain owing to the brittleness of ZnO as compared to PMMA. Meanwhile, volume shrinkage of the ZnO resin caused a reduction in the line width of the isolated free-standing ZnO nanowires from 200 to 115 nm following calcination at 300 °C for 60 min.

Free-Standing Polymer Nanomembrane. Free-standing nanomembranes are very promising for use as nano shadow masks[43] in the fabrication of high-aspect ratio nanostructures or as stencil masks[44,45] for plasmonic biosensing applications. Various types of porous nanomembranes were fabricated under different NTMonMT processing conditions (Figure 6). At a constant pressure and trench depth, free-standing Type A nanomembrane structures formed at low temperature on narrow gap trenches (Figure 6a). At elevated temperature, Type B and D (Figure 6b, d) patterns resulted when gaps of intermediate dimensions were employed. Type C was observed for depositions on shallow wide trenches (Figure 6c). If the transfer process was performed at a temperature above the T_g of PMMA, slightly elongated hole patterns were often observed at the contact region of the top surface and the edge of the trench, as shown in images a and c in Figure 6. In Type C, large elongated hole patterns were observed between the bottom surface and the edge of the trench due to bending and deformation of the PMMA film that occurs at temperatures above the polymer T_g. The resulting pattern types are thus

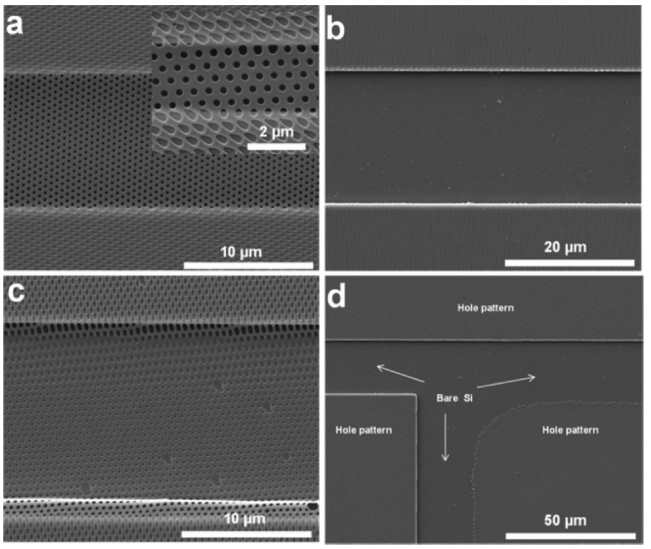

Figure 6. SEM images of various types of porous polymer membrane prepared by NTMonMT. (a) Free-standing nanomembrane with nanohole patterns (Type A for Figure 2) on silicon trenches with 10 μm gaps and 2 μm gaps (inset image) and depths of 0.7 μm deposited by NTM at a temperature of 110 °C. (b) PMMA patterns (Type B) of Figure 2 selectively transferred onto the protruding regions of the silicon trenches with 20 μm gaps at a process temperature of 150 °C. (c) PMMA patterns (Type C) in contact with a recessed area at the bottom of the trenches with 15 μm gaps at a process temperature of 130 °C. (d) Complex PMMA patterns (Type D) including partially nontransferred regions near the edge of the silicon trenches at a process temperature of 150 °C. In each case, the depth of the silicon trenches was about 0.7 μm and the transfer printing pressure was 6 bar applied for a duration of 2 min.

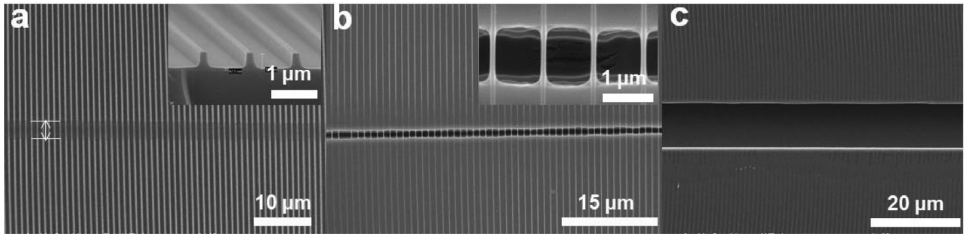

Figure 5. SEM images of (a) Type A ZnO nanoline patterns with a thin residual layer prepared by NTMonMT on 2 μm gaps. Inset shows a cross-sectional image. (b) Isolated ZnO nanowires after thermal annealing at 300 °C for 60 min in a muffle furnace. Inset is enlarged image of b. (c) Type B ZnO patterns prepared by NTMonMT on 15 μm gaps. The depth of the silicon trenches was 2.5 μm.

Table 1. Summary of Dominant Pattern Types with Pressure, Temperature, And Pattern Dimensions[a]

		high pressure (20 bar)				low pressure (6 bar)			
		shallow trench		deep trench		shallow trench		deep trench	
		W	N	W	N	W	N	W	N
PMMA transfer	low T (90 °C below T_g)	C&B	A	B&A	A	A&C	A	A	A
	high T (150 °C)	D&B	B	B&D	B	C&B&D	A	B	A

[a]W, wide gap trench; N, narrow gap trench; A, A type; B, B type; C, C type; D, D type.

affected by the trench dimensions as well as the processing temperature and pressure (see Figures S1−S3 in the Supporting Information). At a high pressure of 20 bar and a temperature of 90 °C, Type C patterns were predominantly obtained except for when narrow gaps (2 μm) were employed. In the transfer of PMMA patterns with nanoholes, Type A patterns dominated at low temperature and low pressure. Types B and D were dominant at high temperature and high pressure, and Type C was observed when wide and shallow trenches were employed at relatively low pressure. Generally, the pattern types obtained with NTMonMT depend on the film thickness, the material's mechanical properties such as toughness, stiffness, and brittleness, pattern dimensions such as gap width and depth, and processing conditions such as temperature and pressure (see Table 1). To investigate a theoretical mechanism about the reason why the different type could be obtained, we completed finite element analysis (FEA) (Figure 7). As shown in Figure 7, deflection of polymer mold is

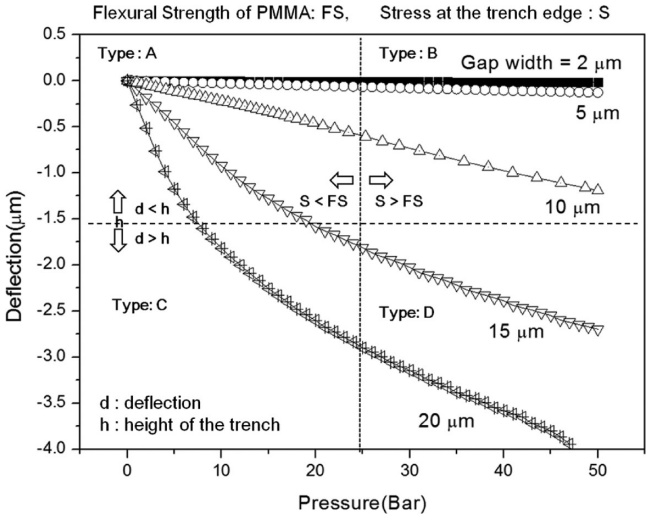

Figure 7. Simulation results of finite element analysis (FEA): deflection with the variation in pressure and gap width.

increased when the gap width gets wider. If the deflection depth (d) is larger than the height of the trench (h), PMMA will contact with the bottom of Si trench and the deflection can lead to Type C or D by applying high pressure over the trench with relatively large gap width. Type B structures are related to the stress localization at the trench edge. If the localized stress at the edge (S) is larger than the flexural strength of PMMA (FS), selective transfer (Type B) will occur because the localized stress above a critical point might induce plastic deformation or crack (see also Figures S4 and S5 in the Supporting Information for additional FEA results).

3D Metal Dot Arrays Using Free-Standing Shadow Mask. A free-standing PMMA nanomembrane with a hole diameter of 265 nm prepared by NTMonMT using 10 μm gap trenches (Figure 8b) was employed as a nanoshadow mask for

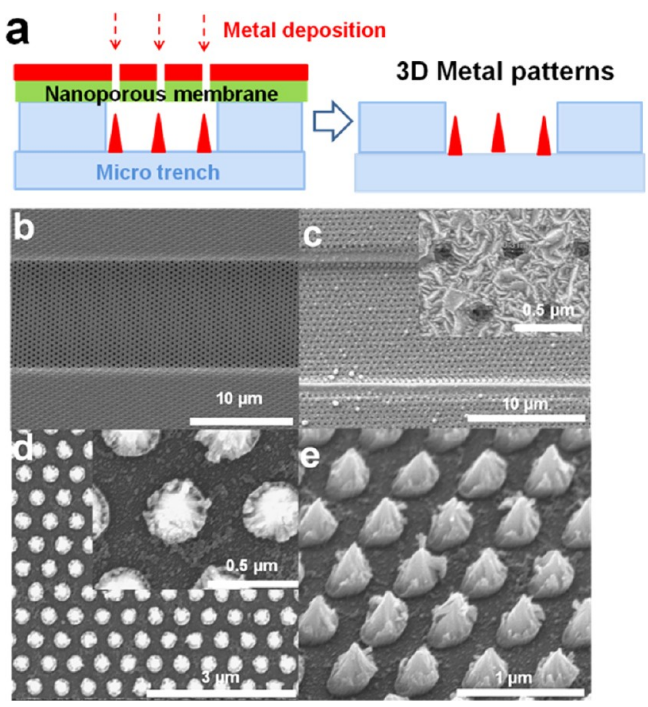

Figure 8. (a) Fabrication scheme of 3D metal dot array using free-standing nanomembrane. (b) SEM image of free-standing PMMA nanomembrane with 265 nm hole diameters on trenches with 10 μm gaps. (c) SEM image of the surface deposited with chromium(Cr) of thickness of 500 nm. (d, e) Plane and tilted SEM images of Cr metal dot arrays with a 3D pyramidal shape after removal of the PMMA membrane, respectively. Inset images of c and d are enlarged images of c and d.

the fabrication of 3D metal arrays. Chromium(Cr) was deposited on the porous polymer mask to a thickness of 500 nm (Figure 8b). The surface of the polymer membrane roughened after Cr deposition and the membrane hole size was reduced from 265 to 100 nm at the surface due to the clogging of membrane holes by the thick metal layer (Figure 8c). The shape of 3D Cr dots was found to be pyramidal (i.e., peaked hat shape) with sharp tips. The average diameter and height of the Cr metal dot arrays were 320 and 420 nm, respectively (Figure 8d, e). The diameter of the base of the dot was larger than the polymer mask hole diameter of 265 nm, because of diffusion effects operative during metal deposition. These complex 3D metal dot arrays in the micro trenches can be applicable to chemical and biological sensor using surface-enhanced Raman scattering (SERS)[46,47] and a high-performance FET structures based on metal dots within microelectrodes to align nanotubes or nanowires.[48]

CONCLUSIONS

In conclusion, we have demonstrated the fabrication of free-standing nanowires and porous nanomembranes using the state-of-the-art NTMonMT nanofabrication process. Perfectly aligned polymer nanowires with sub-100 nm diameter and inorganic (ZnO) nanowires were successfully prepared on microtrenches by NTMonMT. Various transfer patterns were obtained on the trenches including a continuous free-standing film, a selectively transferred structure on the surface of the trenches, and a continuous nanostructured film with recessed areas. The type of pattern generated depended on the dimensions of the trenches as well as the temperature and pressure conditions employed in the NTMonMT process. 3D pyramidal metal (Cr) dot arrays, typically inaccessible by conventional lift-off processes, were successfully fabricated using a free-standing porous nanomembrane. Finally, we believe that the proposed NTMonMT process will be very useful for direct nanoscale manipulation of functional materials on patterned surfaces as well as for the generation of unique 3D structures and our work will be broadly applicable to laterally aligned free-standing nanodevices such as nanoresonators, strain or stress sensors, nanoswitches, FETs, and chemical or biological sensors.

ASSOCIATED CONTENT

Supporting Information

The SEM images on the various process conditions (Figures S1–S3) and details on FEA and additional FEA results (Figures S4 and S5). This material is available free of charge via the Internet at http://pubs.acs.org.

AUTHOR INFORMATION

Corresponding Author

*Address: Nano-Mechanical Systems Research Division, Korea Institute of Machinery & Materials (KIMM), 171 Jang-dong, Yuseong-gu, Daejeon, 305-343, Republic of Korea. Tel: +82-42-868-7846. Fax: +82-42-868-7721. E-mail: lamcdg@kimm.re.kr.

Notes

The authors declare no competing financial interest.

ACKNOWLEDGMENTS

This research was supported by KIMM research funds (NK169D and SC0890) and a NRF grant (2011-0028585 and 2012-0006201).

REFERENCES

(1) Guo, L. J. *Adv. Mater.* **2007**, *19*, 495–513.
(2) Suh, K. Y.; Lee, H. H. *Adv. Funct. Mater.* **2002**, *12*, 405–413.
(3) Zaumseil, J.; Meitl, M. A.; Hsu, J. W. P.; Acharya, B. R.; Baldwin, K. W.; Loo, Y. L.; Rogers, J. A. *Nano Lett.* **2003**, *3*, 1223–1227.
(4) Meitl, M. A.; Zhu, Z. T.; Kumar, V.; Lee, K. J.; Feng, X.; Huang, Y. Y.; Adesida, I.; Nuzzo, R. G.; Rogers, J. A. *Nat. Mater.* **2006**, *5*, 33–38.
(5) Lee, B. H.; Cho, Y. H.; Lee, H.; Lee, K. D.; Kim, S. H.; Sung, M. M. *Adv. Mater.* **2007**, *19*, 1714–1718.
(6) Hwang, J. K.; Cho, S.; Dang, J. M.; Kwak, E. B.; Song, K.; Moon, J.; Sung, M. M. *Nat. Nanotechnol.* **2010**, *5*, 742–748.
(7) Gou, H. L.; Xu, J. J.; Xia, X. H.; Chen, H. Y. *ACS Appl.Mater. Interfaces* **2010**, *2*, 1324–1330.
(8) Packard, C. E.; Murarka, A.; Lam, E. W.; Schmidt, M. A.; Bulovic, V. *Adv. Mater.* **2010**, *22*, 1840–1844.
(9) Hampton, M. J.; Williams, S. S.; Zhou, Z.; Nunes, J.; Ko, D. H.; Templeton, J. L.; Samulski, E. T.; DeSimone, J. M. *Adv. Mater.* **2008**, *20*, 2667–2673.
(10) Park, S. I.; Xiong, Y.; Kim, R. H.; Elvikis, P.; Meitl, M.; Kim, D. H.; Wu, J.; Yoon, J.; Chang-Jae, Y.; Liu, Z.; Huang, Y.; Hwang, K. C.; Ferreira, P.; Xiuling, L.; Choquette, K.; Rogers, J. A. *Science* **2009**, *325*, 977–981.
(11) Kim, S.; Wu, J.; Carlson, A.; Jin, S. H.; Kovalsky, A.; Glass, P.; Liu, Z.; Ahmed, N.; Elgan, S. L.; Chen, W.; Ferreira, P. M.; Sitti, M.; Huang, Y.; Rogers, J. A. *Proc. Natl. Acad. Sci. U. S. A.* **2010**, *107*, 17095–17100.
(12) Park, K. I.; Xu, S.; Liu, Y.; Hwang, G. T.; Kang, S. J. L.; Wang, Z. L.; Lee, K. J. *Nano Lett.* **2010**, *10*, 4939–4943.
(13) Ko, H.; Takei, K.; Kapadia, R.; Chuang, S.; Fang, H.; Leu, P. W.; Ganapathi, K.; Plis, E.; Kim, H. S.; Chen, S. Y.; Madsen, M.; Ford, A. C.; Chueh, Y. L.; Krishna, S.; Salahuddin, S.; Javey, A. *Nature* **2010**, *468*, 286–289.
(14) Yang, Y.; Hwang, Y.; Cho, H. A.; Song, J. H.; Park, S. J.; Rogers, J. A.; Ko, H. C. *Small* **2011**, *7*, 484–491.
(15) Choi, D.-G.; Lee, K.-J.; Kim, S.; Lee, E.-S.; Jeong, J.-H.; Lee, J.; Choi, J.-H. *RSC Adv.* **2012**, *2*, 11035–11039.
(16) Huang, X. D.; Bao, L. R.; Cheng, X.; Guo, L. J.; Pang, S. W.; Yee, A. F. *J. Vac. Sci. Technol. B* **2002**, *20*, 2872–2876.
(17) Tan, L.; Kong, Y. P.; Bao, L. R.; Huang, X. D.; Guo, L. J.; Pang, S. W.; Yee, A. F. *J. Vac. Sci. Technol. B* **2003**, *21*, 2742–2748.
(18) Suh, D.; Choi, S. J.; Lee, H. H. *Adv. Mater.* **2005**, *17*, 1554–1560.
(19) Dumond, J.; Low, H. Y. *Adv. Mater.* **2008**, *20*, 1291–1297.
(20) Chen, L.; Degenaar, P.; Bradley, D. D. C. *Adv. Mater.* **2008**, *20*, 1679–1683.
(21) Lee, D. Y.; Hines, D. R.; Stafford, C. M.; Soles, C. L.; Lin, E. K.; Oehrlein, G. S. *Adv. Mater.* **2009**, *21*, 2524–2529.
(22) Jeong, J. W.; Park, W. I.; Do, L. M.; Park, J. H.; Kim, T. H.; Chae, G.; Jung, Y. S. *Adv. Mater.* **2012**, *24*, 3526–3531.
(23) Yim, K. H.; Zheng, Z.; Liang, Z.; Friend, R. H.; Huck, W. T. S.; Kim, J. S. *Adv. Funct. Mater.* **2008**, *18*, 1012–1019.
(24) Ko, D. H.; Tumbleston, J. R.; Zhang, L.; Williams, S.; DeSimone, J. M.; Lopez, R.; Samulski, E. T. *Nano Lett.* **2009**, *9*, 2742–2746.
(25) Wang, D. H.; Choi, D. G.; Lee, K. J.; Park, O. O.; Park, J. H. *Langmuir* **2011**, *26*, 9584–9588.
(26) Wang, D. H.; Choi, D. G.; Lee, K. J.; Park, O. O.; Park, J. H. *Org. Electron.* **2010**, *11*, 599–603.
(27) Kim, H.; Yoon, B.; Sung, J.; Choi, D. G.; Park, C. *J. Mater. Chem.* **2008**, *18*, 3489–3495.
(28) Lee, T. W.; Zaumseil, J.; Bao, Z.; Hsu, J. W. P.; Rogers, J. A. *Proc. Natl. Acad. Sci. U.S.A.* **2004**, *101*, 429–433.
(29) Kang, D.; Pang, C.; Kim, S. M.; Cho, H. S.; Um, H. S.; Choi, Y. W.; Suh, K. Y. *Adv. Mater.* **2012**, *24*, 1709–1715.
(30) Park, S. H.; Jeong, J. H.; Choi, D. G.; Kim, K. D.; Altun, A. O.; Lee, E. S.; Yang, D. Y.; Lee, K. S. *Appl. Phys. Lett.* **2007**, *90*, 233109.
(31) Lee, C.; Wei, X.; Kysar, J. W.; Hone, J. *Science* **2008**, *321*, 385–388.
(32) Berciaud, S.; Ryu, S.; Brus, L. E.; Heinz, T. F. *Nano Lett.* **2009**, *9*, 346–352.
(33) Fei, P.; Yeh, P. H.; Zhou, J.; Xu, S.; Gao, Y.; Song, J.; Gu, Y.; Huang, Y.; Wang, Z. L. *Nano Lett.* **2009**, *9*, 3435–3439.
(34) Bak, J. H.; Kim, Y. D.; Hong, S. S.; Lee, B. Y.; Lee, S. R.; Jang, J. H.; Kim, M.; Char, K.; Hong, S.; Park, Y. D. *Nat. Mater.* **2008**, *7*, 459–463.
(35) Bunch, J. S.; Van Der Zande, A. M.; Verbridge, S. S.; Frank, I. W.; Tanenbaum, D. M.; Parpia, J. M.; Craighead, H. G.; McEuen, P. L. *Science* **2007**, *315*, 490–493.
(36) Khaderbad, M. A.; Choi, Y.; Hiralal, P.; Aziz, A.; Wang, N.; Durkan, C.; Thiruvenkatanathan, P.; Amaratunga, G. A. J.; Rao, V. R.; Seshia, A. A. *Nanotechnology* **2012**, *23*, 025501.
(37) Long, R.; Chen, J.; Lim, J. H.; Wiley, J. B.; Zhou, W. *Nanotechnology* **2009**, *20*, 285306.

(38) Freer, E. M.; Grachev, O.; Duan, X.; Martin, S.; Stumbo, D. P. *Nat. Nanotechnol.* **2010**, *5*, 525−530.
(39) Liu, X.; Long, Y. Z.; Liao, L.; Duan, X.; Fan, Z. *ACS Nano* **2012**, *6*, 1888−1900.
(40) Lee, C. H.; Kim, D. R.; Zheng, X. *Nano Lett.* **2011**, *11*, 3435−3439.
(41) Lee, C. H.; Kim, D. R.; Zheng, X. *Proc. Natl. Acad. Sci. U.S.A.* **2010**, *107*, 9950−9955.
(42) Kim, S.; Shin, D. O.; Choi, D. G.; Jeong, J. R.; Mun, J. H.; Yang, Y. B.; Kim, J. U.; Kim, S. O.; Jeong, J. H. *Small* **2012**, *8*, 1563−1569.
(43) Kim, Y. C.; Lee, S. S. *J. Micromech. Microeng.* **2008**, *18*, 015006.
(44) Vazquez-Mena, O.; Sannomiya, T.; Villanueva, L. G.; Voros, J.; Brugger, J. *ACS Nano* **2011**, *5*, 844−853.
(45) Vazquez-Mena, O.; Sannomiya, T.; Tosun, M.; Villanueva, L. G.; Savu, V.; Voros, J.; Brugger, J. *ACS Nano* **2012**, *6*, 5474−5481.
(46) Heo, C. J.; Kim, S. H.; Jang, S. G.; Lee, S. Y.; Yang, S. M. *Adv. Mater.* **2009**, *21*, 1726−1731.
(47) Jeon, H. C.; Heo, C. J.; Lee, S. Y.; Yang, S. M. *Adv. Funct. Mater.* **2012**, *22*, 4268−4274.
(48) Jeon, H. J.; Baek, Y. K.; Yang, S. B.; Lee, S. K.; Jung, J. M.; Jung, H. T. *J. Mater. Chem.* **2011**, *21*, 14285−14290.